British Journal of Pharmacology (2002) 136, 1015–1022

www.nature.com/bjp

Characterization of G proteins involved in activation of nonselective cation channels by endothelin$_B$ receptor

*,[1,2]Yoshifumi Kawanabe, [1]Nobuo Hashimoto & [2]Tomoh Masaki

[1]Department of Neurosurgery, Kyoto University Faculty of Medicine, Sakyo-ku, Kyoto 606-8507, Japan and [2]Department of Pharmacology, Kyoto University Faculty of Medicine, Sakyo-ku, Kyoto 606-8507, Japan

1 We recently demonstrated that endothelin-1 (ET-1) activates two types of Ca^{2+}-permeable nonselective cation channels (NSCC-1 and NSCC-2) in Chinese hamster ovary cells expressing endothelin$_B$ receptors (CHO-ET$_B$R) that couple with G_q and G_i. The purpose of the present study was to identify the G proteins involved in the activation of these Ca^{2+} channels by ET-1. For this purpose, we constructed CHO cells expressing an unpalmitoylated ($Cys^{402}Cys^{403}$ Cys^{405}→$Ser^{402}Ser^{403}$-Ser^{405}) ET$_B$R (CHO-SerET$_B$R) and ET$_B$R truncated at the cytoplasmic tail downstream of Cys^{403} (CHO-ET$_B$RΔ403).

2 Based on the data obtained from actin stress fibre formation, CHO-ET$_B$R couple with G_{13}. Therefore, CHO-ET$_B$R couple with G_q, G_i and G_{13}. CHO-SerET$_B$R and CHO-ET$_B$RΔ403 couple with G_{13} and G_q, respectively.

3 ET-1 activated NSCC-1 in CHO-ET$_B$R preincubated with phospholipase C (PLC) inhibitor, U73122, and in CHO-SerET$_B$R. On the other hand, ET-1 failed to activate Ca^{2+} channels in CHO-ET$_B$RΔ403. Microinjection of dominant negative mutants of G_{13} (G_{13}G225A) abolished activation of NSCC-1 and NSCC-2 in CHO-ET$_B$R and that of NSCC-1 in CHO-SerET$_B$R.

4 Y-27632, a specific Rho-associated kinase (ROCK) inhibitor, did not affect the ET-1-induced transient and sustained increase in $[Ca^{2+}]_i$ in CHO-ET$_B$R.

5 These results indicate that (1) the cytoplasmic tail downstream of the palmitoylation sites of ET$_B$R, but not the palmitoylation site itself, is essential for coupling with G_{13}, (2) the activation mechanism of each Ca^{2+} channel by ET-1 is different in CHO-ET$_B$R. NSCC-1 activation depends on G_{13}-dependent cascade, and NSCC-2 activation depends on both G_q/PLC- and G_{13}-dependent cascades. Moreover, ROCK-dependent cascade is not involved in the activation of these channels. *British Journal of Pharmacology* (2002) **136,** 1015–1022

Keywords: Endothelin; endothelin$_B$ receptor; G protein; actin stress-fibre formation; nonselective cation channel

Abbreviations: $[Ca^{2+}]_i$; intracellular free Ca^{2+} concentration; CHO-ET$_B$R, Chinese hamster ovary cells that stably express human endothelin$_B$ receptor; CHO-ET$_B$RΔ403, Chinese hamster ovary cells that express human endothelin$_B$ receptor truncated at the carboxyl-terminal downstream of Cys403; CHO-SerET$_B$R, Chinese hamster ovary cells that express the unpalmitoylated ($Cys^{402}Cys^{403}$ Cys^{405} → $Ser^{402}Ser^{403}$ Ser^{405}) human endothelin$_B$ receptor; ET-1, endothelin-1; FCS, foetal calf serum; F_{max}, fluorescence intensity maximum; F_{min}, fluorescence intensity minimum; G_{12}G228A, dominant negative type of G_{12}; G_{13}G225A, dominant negative type of G_{13}; GPCR, heterotrimetric guanine nucleotide-binding protein (G-protein)-coupled receptor; NSCC, nonselective cation channel; IPs, inositol phosphates; PBS, phosphate-buffered saline; PBS-Tx, phosphate-buffered saline containing 0.1% Triton-X100; PLC, phospholipase C; PTX, pertussis toxin; ROCK, Rho-associated kinase; U73122, 1-(6-{[17β-3-methoxyestra-1,3,5(10)-trien-17-yl] amino}hexyl)-1H-pyrrole-2,5-dione; VICC, voltage-independent Ca^{2+} channel; Y-27632, (R)-(+)-trans-N-(4-pyridyl)-4-(1-aminoethyl)-cyclohexanecarboxamide

Introduction

Endothelin-1 (ET-1) has a wide variety of biological effects on various tissues and cell types (Yanagisawa *et al*., 1988; Masaki, 1993) that are mediated by specific heterotrimetric guanine nucleotide-binding protein (G-protein)-coupled receptor (GPCR) subtypes, the endothelin$_A$ receptor (ET$_A$R) and endothelin$_B$ receptor (ET$_B$R) (Arai *et al*., 1990; Sakurai *et al*., 1990). When expressed in Chinese hamster ovary (CHO) cells, ET$_A$R couples with members of the G_q and G_s families and stimulates phospholipase C (PLC) and adenylyl cyclase, respectively. ET$_B$R couples with members of the G_q and G_i families and stimulates PLC and inhibits adenylyl cyclase, respectively (Aramori & Nakanishi, 1992; Takagi *et al*., 1995). Many GPCRs including ET$_A$R and ET$_B$R were shown to be palmitoylated at a cluster of cysteine residues located in the cytoplasmic tail (Horstmeyer *et al*., 1996; Okamoto *et al*., 1997). The functional role of palmitoylation and the cytoplasmic tail downstream of the palmitoylation site in coupling with G proteins has been studied for ET$_A$R and ET$_B$R in some detail. In the case of ET$_B$R, palmitoylation is essential for coupling of the receptor with both G_q and G_i, while the cytoplasmic tail downstream of the palmitoylation sites is also required for coupling with G_i (Okamoto *et al*., 1997). It is reported that both ET$_A$R and ET$_B$R can also couple with the G_{12} subfamily,

*Author for correspondence at: Membrane Biology Program, Brigham and Women's Hospital, Harvard Institute of Medicine, Room 520, 77 Avenue Louis Pasteur, Boston, Massachusetts, MA 02115, U.S.A.; E-mail: ykawanabe@rics.bwh.harvard.edu

consisting of G_{12} and G_{13}, in NIH3T3 cells (Mao *et al*., 1998). The G_{12} subfamily has been shown to mediate important signaling pathways such as Rho/Rho-associated kinase (ROCK)-dependent formation of actin stress fibres (Buhl *et al*., 1995) and vascular smooth muscle cell contraction (Gohla *et al*., 2000). These reports suggested that the G_{12} subfamily may play important roles in several ET-1-induced vascular disorders such as stroke or vasospasm. Thus, the control of G_{12} subfamily activation may become a new treatment strategy for these conditions. Recently, it was shown that upon treatment with ET-1, ET_BR in fibroblast cell lines did not induce stress fiber formation (Gohla *et al*., 1999), whereas ET_BR in HEK 293 cells coupled to G_{13} (Kitamura *et al*., 1999). These data imply that in some types of cells, stimulation of ET_BR can induce actin stress fibre formation *via* a member of G_{12} family, although direct evidence is absent. Therefore, in the present study, we attempt to determine whether stimulation of ET_BR actually induces actin stress fibre formation in CHO cells expressing recombinant ET_BR (CHO-ET_BR), and if so, which subtypes of G proteins are involved in the formation. Furthermore, we analyse the domains of ET_BR that are necessary for coupling of the receptor with the G protein. For these purposes, we use dominant negative mutants of G_{12} and G_{13} as well as mutated ET_BRs that lose the ability to couple with G_q and/or G_i. Previous report demonstrated that CHO cells expressing ET_BR truncated at the cytoplasmic tail downstream of Cys^{403} (CHO-$ET_BR\Delta403$) coupled with G_q but not with G_i, whereas CHO cells expressing the unpalmitoylated ($Cys^{402}Cys^{403}Cys^{405}\rightarrow Ser^{402}Ser^{403}Ser^{405}$) ET_BR (CHO-SerET_BR) coupled with neither G_q nor G_i (Okamoto *et al*., 1997).

Recent reports demonstrated that ET-1-induced extracellular Ca^{2+} influx through voltage-independent Ca^{2+} channels (VICCs) plays a critical role for ET-1-induced vasoconstriction and cell proliferation (Zhang *et al*., 1999; Kawanabe *et al*., 2002). Thus, it is important to elucidate the activation mechanisms of VICCs by ET-1. We focused on investigating which G-protein subtypes were involved in activation of each Ca^{2+} channel by ET-1 in CHO-ET_BR. Transfection and functional expression of the cDNA clone for wild type or mutant ET_BRs into the same cell type provide a model system to study the precise characteristics of signal transduction by a single receptor subtype. We used CHO cells stably expressing wild-type or mutant ET_BRs in the present study. A recent report showed that ET-1 activates two types of Ca^{2+}-permeable nonselective cation channels (designated NSCC-1 and NSCC-2) in CHO-ET_BR (Kawanabe *et al*., 2001). In particular, these channels can be distinguished using Ca^{2+} channel blockers, SK&F 96365 and LOE 908. Thus, NSCC-1 is sensitive to LOE 908 and resistant to SK&F 96365, whereas NSCC-2 is sensitive to both LOE 908 and SK&F 96365 (Kawanabe *et al*., 2001). In the present study, we used a dominant negative mutant of G_{13} and two types of mutated ET_BRs designated $ET_BR\Delta403$ and SerET_BR to clarify the involvement of G_q, G_I and G_{13} for Ca^{2+} channel activation by ET-1.

Methods

Mutagenesis

Wild-type G_{12} and G_{13} in pcDNA3(+) were kindly provided by Dr Manabu Negishi (Kyoto University, Japan). G_{12}G228A and G_{13}G225A, which were shown to be the dominant negative types (Gohla *et al*., 1999), were generated using the QuickChange™ site-directed mutagenesis kit (Stratagene, La Jolla, CA, U.S.A.). Mutations were verified by sequencing.

Cell culture

We used CHO-ET_BR, CHO-$ET_BR\Delta403$ and CHO-SerET_BR, which were constructed as described previously (Okamoto *et al*., 1997). The K_D and B_{max} values of selected cell clones that were used in this study were 43 ± 3 pM and 0.98 ± 0.11 pmol (mg protein)$^{-1}$, respectively, for CHO-ET_BR; 122 ± 10 pM and 1.66 ± 0.12 pmol (mg protein)$^{-1}$, respectively, for CHO-$ET_BR\Delta403$; and 38 ± 3 pM and 1.29 ± 0.10 pmol (mg protein)$^{-1}$, respectively, for CHO-SerET_BR. Cells were maintained in Ham's F-12 medium supplemented with 10% foetal calf serum (FCS) under a humidified 5% CO_2/95% air atmosphere.

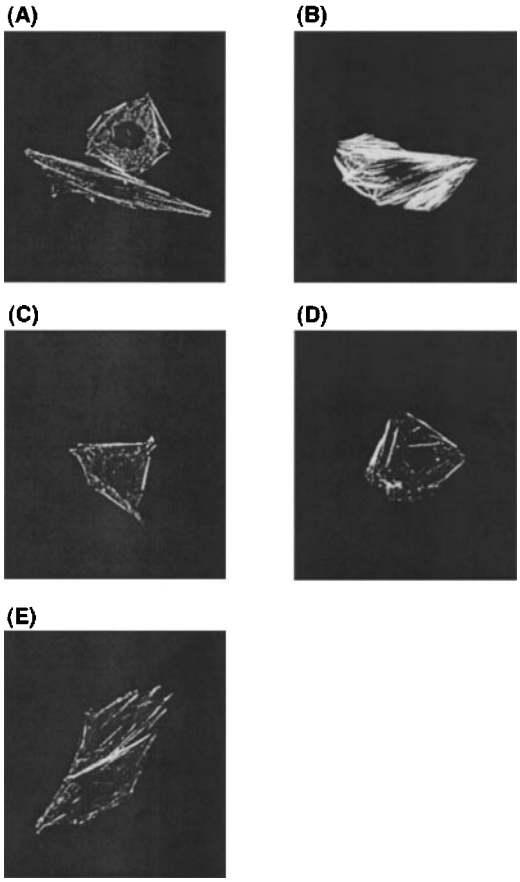

Figure 1 Effects of Y-27632, U73122, G_{12}G228A and G_{13}G225A on the ET-1-induced actin stress fibre formation in CHO-ET_BR. Cells were stimulated with (B~E) or without (A) 10 nM ET-1. The effects of preincubation with 10 μM Y-27632 (C), combination of G_{13}G225A microinjection and 5 μM U73122 preincubation (D) and combination of G_{13}G228A microinjection, PTX (50 ng ml^{-1}) preincubation and 5 μM U73122 preincubation (E) on ET-1-induced stress fibre formation are shown. Y-27632, U73122 and PTX were added 15 min before stimulation with ET-1. Expression plasmids encoding for G_{12}G228A and G_{13}G225A were microinjected into the cell nuclei 24 h before stimulation with ET-1. Actin stress fibers were visualized as described in Methods. Representative examples of stress fibres in individual cells are shown.

Microinjection

For microinjection, cells were seeded onto glass coverslips coated with fibronectin (Iwaki glass, Chiba, Japan), which were marked with a cross to facilitate the localization of injected cells, and incubated overnight in Ham's F-12 medium containing 1% FCS. Plasmids (100 ng μl^{-1}) encoding for G_{12}G228A and G_{13}G225A were microinjected into cell nuclei. As a control, expression plasmids without inserts were microinjected in an adjacent field on the same coverslip. Microinjection was performed using a manual microinjection system (Eppendorf, Hamburg, Germany) equipped with an Axiovert 100 inverted microscope (Carl-Zeiss, Frankfurt, Germany).

Stress fiber formation

After incubation of the cells with serum-free Ham's F-12 medium for 24 h, ET-1 was added at 37°C for 5 min. Cells were washed three times with phosphate-buffered saline (PBS) and fixed with 4% paraformaldehyde in PBS at room temperature for 15 min. After being washed five times with PBS containing 0.1% Triton-X100 (PBS-Tx), the cells were incubated with fluorescein rhodamin-phalloidin (Molecular Probes, Eugene, OR, U.S.A.) in PBS-Tx (1 : 200) at room temperature for 10 min. After being washed five times with PBS-Tx, the labeled cells were mounted on glass slides and examined with an MRC 1024 laser-scanning confocal microscope (Bio-Rad, Hercules, CA, USA) equipped with an Axiovert 135 M inverted microscope (Carl-Zeiss, Frankfurt, Germany).

Measurement of intracellular free Ca^{2+} concentration ($[Ca^{2+}]_i$)

$[Ca^{2+}]_i$ was measured using a fluorescent probe fluo-3. The measurement of fluorescence by a CAF 110 spectrophotometer (JASCO, Tokyo, Japan) was performed exactly as described in a previous report (Kawanabe *et al*., 2001).

Microfluorimetry of fluo-3 was done as described previously (Zhang *et al*., 1999). Briefly, the cells were seeded on 35-mm glass-bottomed plastic dishes (MatTek Corporation, Ashland MA, U.S.A.), which were marked with a cross to facilitate the localization of injected cells, were loaded with fluo-3 by incubating them with Ca^{2+}-free Krebs-HEPES solution containing 10 μM fluo-3/AM for 30 min at 37°C

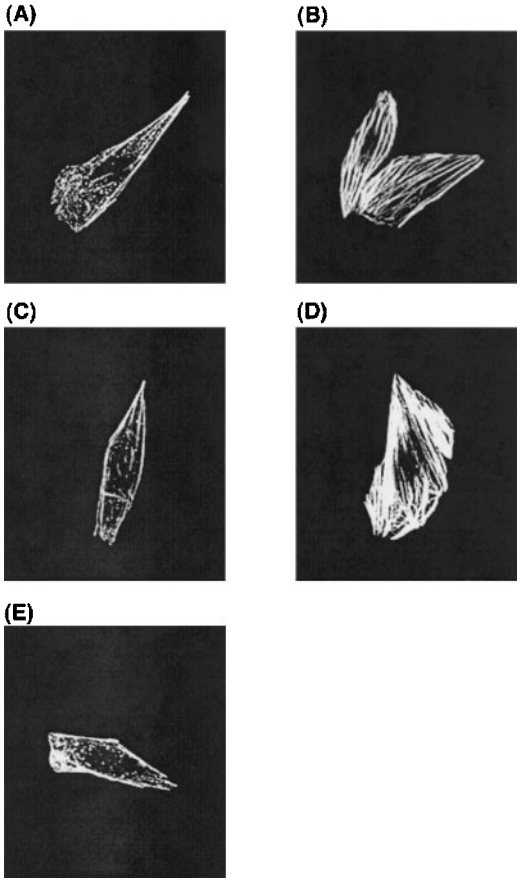

Figure 2 Effects of Y27632, G_{12}G228A and G_{13}G225A on ET-1-induced actin stress fiber formation in CHO-SerET_BR. Cells were stimulated with (B∼E) or without (A) 10 nM ET-1. (C) Y-27632 at 10 μM was added 15 min before stimulation with ET-1. Expression plasmids encoding for G_{12}G228A (D) and G_{13}G225A (E) were microinjected into cell nuclei 24 h before stimulation with ET-1. Actin stress fibres were visualized as described in Methods. Representative examples of stress fibres in individual cells are shown.

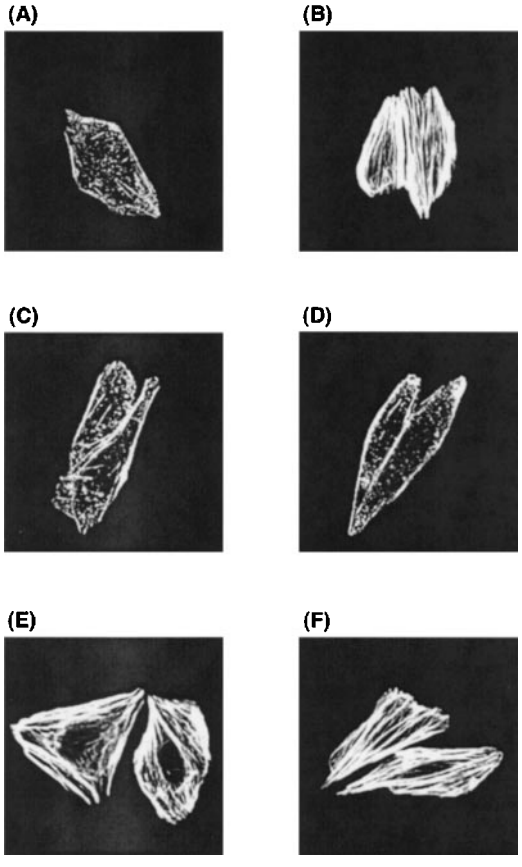

Figure 3 Effects of Y27632, U73122, G_{12}G228A and G_{13}G225A on ET-1-induced actin stress fiber formation in CHO-$ET_BR\Delta$403. Cells were stimulated with (B∼F) or without (A) 10 nM ET-1. Y-27632 at 10 μM (C) and U73122 at 5 μM (D) were added 15 min before stimulation with ET-1. Expression plasmids encoding G_{12}G228A (E) and G_{13}G225A (F) were microinjected into the cell nuclei 24 h before stimulation with ET-1. Actin stress fibres were visualized as described in Methods. Representative examples of stress fibres in individual cells are shown.

under a reduced light. Ca^{2+}-free Krebs-HEPES solution contained (in mM): NaCl 140, KCl 3, $MgCl_2$ 1, glucose 11 and HEPES 10 (pH 7.4, adjusted with NaOH). After washing with Krebs-HEPES solution (2.2 mM $CaCl_2$ was added to Ca^{2+}-free Krebs-HEPES solution), they were kept in fresh Krebs-HEPES solution at 37°C for at least 30 min. Fluo-3 microfluorimetry was done at 25°C by an Attofluor Ratio-Vision real-time digital fluorescence analyser (Atto Instruments, Potomac, MD, U.S.A.) equipped with a Carl-Zeiss Axiovert-100 inverted epifluorescent microscope. A 100-W mercury burner served as the source of excitation. In measurement of $[Ca^{2+}]_i$, fluo-3 was excited at 450–490 nm and fluorescence was detected at 515–565 nm. At the end of the experiment, ionomycin and subsequently EGTA were added at final concentrations of 10 μM and 10 mM, respectively, to obtain the fluorescence intensity maximum (F_{max}) and the fluorescence intensity minimum (F_{min}). $[Ca^{2+}]_i$ was determined from the equilibrium equation, $[Ca^{2+}]_i = K_d(F - F_{min})/(F_{max}-F)$, where F was the experimental value of fluorescence and K_d was defined as 0.4 μM (Minta *et al*., 1989).

Drugs

Boehringer Ingelheim K.G. (Ingelheim, Germany) kindly provided LOE 908. (R)-(+)-trans-N-(4-pyridyl)-4-(1-aminoethyl)-cyclohexanecarboxamide (Y-27632) was kindly provided by Welfide Corporation (Osaka, Japan). Chemicals were obtained from the following sources: ET-1 from the Peptide Institute (Osaka, Japan); rhodamin-phalloidin from Molecular Probes (Eugene, OR, U.S.A.); pertussis toxin and 1-(6-{[17β-3-methoxyestra-1,3,5(10)-trien-17-yl] amino}hexyl)-1H-pyrrole-2,5-dione (U73122) from Funakoshi Co. Ltd (Tokyo, Japan); SK&F 96365 from Biomol (Plymouth Meeting, PA, USA); and fluo-3/AM from Dojindo Laboratories (Kumamoto, Japan). All other chemicals were of reagent grade and were obtained commercially.

Statistical analysis

All results were expressed as mean ± s.e.m.

Results

ET-1-induced actin stress fiber formation in CHO-ET_BR

We attempted to determine the structural basis for coupling of ET_BR with G_{12}/G_{13} and subtypes of G proteins involved in ET-1-induced stress fibre formation. For these purposes, we examined the effects of inhibition of either one of the G protein-mediated signalling cascades by blockers and dominant negative mutants of G_{12} or G_{13} (G_{12}G228A or G_{13}G225A, respectively) on ET-1-induced actin stress fibre formation in CHO-$ET_BR\Delta403$ and CHO-SerET_BR as well as CHO-ET_BR. As described previously (Gohla *et al*., 1999), G_{12}G228A inhibited ET-1-induced actin stress fibre formation in CHO cells expressing endothelin$_A$ receptors (data not shown).

ET-1 induced actin stress fiber formation in CHO-ET_BR (Figure 1B). In contrast, ET-1 failed to induce stress fibre formation in CHO-ET_BR that had been preincubated with 10 μM Y-27632, a selective ROCK inhibitor (Figure 1C). Y-27632 was added 15 min before stimulation with ET-1. Stress fiber formation was not affected by pretreatment with 5 μM

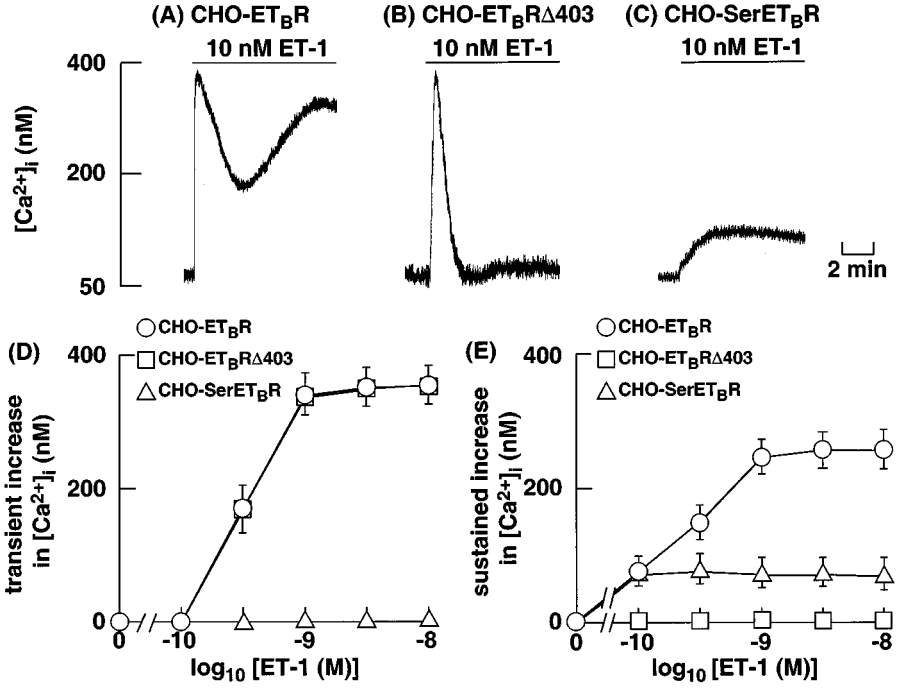

Figure 4 Original tracings illustrating the effects of ET-1 on the increase in $[Ca^{2+}]_i$ in CHO-ET_BR (A), CHO-$ET_BR\Delta403$ (B) and CHO-SerET_BR (C). The cells were loaded with fluo-3 and stimulated with 10 nM ET-1 at the time indicated by arrows. Effects of various concentrations of ET-1 on the transient increase in $[Ca^{2+}]_i$ (D) and the sustained increase in $[Ca^{2+}]_i$ (E) in CHO-ET_BR, CHO-$ET_BR\Delta403$ and CHO-SerET_BR. The values for CHO-ET_BR, CHO-$ET_BR\Delta403$ and CHO-SerET_BR were represented by circles, squares and triangles, respectively. Each point represents the mean ± s.e.m. of five experiments.

U73122, a PLC inhibitor, or microinjection of G_{12}G228A or G_{13}G225A in CHO-ET_BR (data not shown). When the cells were subjected to microinjection of G_{13}G225A followed by pretreatment with U73122, ET-1 failed to induce stress fiber formation (Figure 1D). In contrast, microinjection of G_{12}G228A in combination with pretreatment by U73122 had no effect on ET-1-induced stress fiber formation (data not shown). These results demonstrate that ET_BR couples to G_{13} but not G_{12} in CHO cells.

A previous report demonstrated that, in preadipocytes, α_2-adrenergic receptor activation of Rho was PTX sensitive (Betuing *et al*., 1998). In contrast, the other previous report showed that Rho-mediated effects on the cytoskeleton are PTX insensitive (Buhl *et al*., 1995). Therefore, we tried to clarify whether G_i played roles in ET-1-induced actin stress fibre formation in CHO-ET_BR using pertussis toxin (PTX; 50 ng ml^{-1}). It is generally accepted that PTX inhibits the effects of G_i (Takagi *et al*., 1995). The degree of ET-1-induced stress fiber formation in CHO-ET_BR that had been treated with combination of G_{13}G225A microinjection, PTX preincubation, and U73122 preincubation (Figure 1E) was similar to that in CHO-ET_BR that had been treated with combination of G_{13}G225A microinjection and U73122 preincubation (Figure 1D). These results indicate that G_i may not be involved in ET-1-induced actin stress fiber formation in CHO-ET_BR.

ET-1-induced actin stress fiber formation in CHO-SerET_BR and CHO-$ET_BR\Delta403$

ET-1 induced stress fiber formation in CHO-SerET_BR (Figure 2B). Like CHO-ET_BR, ET-1 induced stress fiber formation was inhibited by preincubation of CHO-SerET_BR with Y-27632 (Figure 2C), but was not affected by microinjection of G_{12}G228A (Figure 2D). Notably, unlike CHO-ET_BR, it was inhibited by microinjection of G_{13}G225A (Figure 2E).

ET-1 induced stress fiber formation in CHO-$ET_BR\Delta403$, in which coupling of the receptor with G_q but not G_i was retained (Figure 3B). Like CHO-ET_BR, ET-1-induced stress fiber formation was inhibited by preincubation of CHO-$ET_BR\Delta403$ with Y-27632 (Figure 3C). Notably, unlike CHO-ET_BR, it was inhibited by preincubation with U73122 (Figure 3D). In contrast, it was not affected by microinjection of G_{12}G228A or G_{13}G225A (Figure 3E,F).

These results indicate that SerET_BR, but not $ET_BR\Delta403$, couples with G_{13}.

Basic properties of the ET-1-induced increase in $[Ca^{2+}]_i$ in CHO-ET_BR, CHO-$ET_BR\Delta403$ and CHO-SerET_BR

ET-1 induced a biphasic increase in $[Ca^{2+}]_i$ in CHO-ET_BR, consisting of an initial transient phase and a subsequent sustained phase (Figure 4A). Both the transient and sustained increase in $[Ca^{2+}]_i$ were dependent on the concentrations of ET-1, and reached the maximal value at concentrations $\geqslant$1 nM (Figure 4D,E).

In CHO-$ET_BR\Delta403$, which are coupled with G_q alone, stimulation with 1 nM ET-1 caused a transient peak but not sustained increase in $[Ca^{2+}]_i$ (Figure 4B). The magnitude of the transient increase in $[Ca^{2+}]_i$ in CHO-$ET_BR\Delta403$ was essentially similar to that in CHO-ET_BR (Figure 4D).

In CHO-SerET_BR, which are coupled with G_{13} (Figure 2), ET-1 failed to induce an initial transient increase in $[Ca^{2+}]_i$, and it induced only a sustained increase in $[Ca^{2+}]_i$ (Figure 4C). The magnitude of the sustained increase in $[Ca^{2+}]_i$ in CHO-SerET_BR was lower than that in CHO-ET_BR (Figure 4E).

Pharmacological identification of Ca^{2+} channels activated by ET-1 in CHO-ET_BR and CHO-SerET_BR

As described previously (Kawanabe *et al*., 2001), in CHO-ET_BR, the ET-1-induced sustained increase in $[Ca^{2+}]_i$ was completely suppressed by the maximally effective concentration (10 μM) of LOE 908, whereas it was partially inhibited by the maximally effective concentration (10 μM) of SK&F 96365 (Figure 5A,B,E). PTX at 50 ng ml^{-1} failed to affect the resting $[Ca^{2+}]_i$ and the ET-1-induced increase in $[Ca^{2+}]_i$ in CHO-ET_BR (data not shown). In CHO-SerET_BR, the ET-1-induced sustained increase in $[Ca^{2+}]_i$ was completely inhibited by 10 μM LOE 908, whereas SK&F 96365 at concentrations up to 10 μM had no effects (Figure 5C,D,F). These results demonstrate that ET-1 activates only NSCC-1 (LOE 908-sensitive and SK&F 96365 resistant) in CHO-SerET_BR.

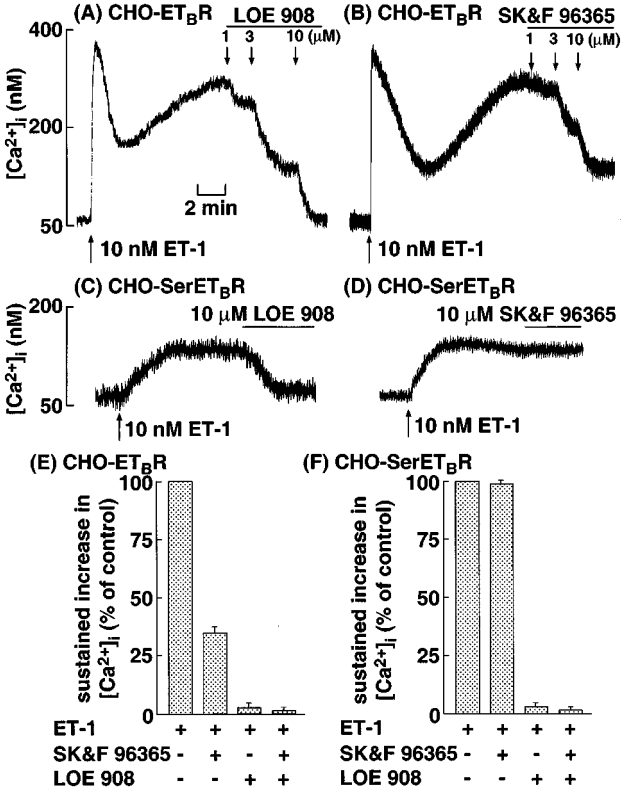

Figure 5 Original tracings illustrating the effects of various concentrations of LOE 908 and SK&F 96365 on the ET-1-induced sustained increase in $[Ca^{2+}]_i$ in CHO-ET_BR (A,B) and CHO-SerET_BR (C,D). The cells were loaded with fluo-3 and stimulated with 10 nM ET-1 at the time indicated by arrows. After $[Ca^{2+}]_i$ reached a steady-state, various concentrations of LOE 908 or SK&F 96365 was added as indicated by arrows. Effects of maximally effective concentration of LOE 908, SK&F 96365 and their combination on the ET-1-induced sustained increase in $[Ca^{2+}]_i$ in CHO-ET_BR (E) and CHO-SerET_BR (F). The experimental protocols were described in Methods, and the values of $[Ca^{2+}]_i$ following addition of 10 μM LOE 908 and/or 10 μM SK&F 96365 were determined. Each point represents the mean$\pm$s.e.m. of five experiments.

Effects of inhibition of PLC on the species of ET-1-activated Ca^{2+} channels in CHO-ET_BR

In CHO-SerET_BR, coupling between the receptor and G_q is missing and hence PLC as an effector of G_q cannot be activated upon stimulation of the receptor. To mimic the stimulation in CHO-SerET_BR and confirm that PLC actually acts as an effector for activation of Ca^{2+} channels, we used U73122 in CHO-ET_BR stimulated by ET-1. ET-1 at 1 nM induced only the sustained increase in $[Ca^{2+}]_i$ in CHO-ET_BR treated with 5 μM U73122 (Figure 6A,B). The magnitude of the sustained increase in $[Ca^{2+}]_i$ was about 35% of that in the absence of U73122 (Figure 6C). This sustained increase in $[Ca^{2+}]_i$ was completely inhibited by 10 μM LOE 908, whereas SK&F 96365 at concentrations up to 10 μM had no effects (Figure 6). These results indicate that ET-1 activates only NSCC-1 in CHO-ET_BR treated with U73122.

Effects of G_{13} on the ET-1-induced sustained increase in $[Ca^{2+}]_i$ in CHO-ET_BR or CHO-SerET_BR

To assess the involvement of G_{13} in the activation of Ca^{2+} channels, we investigated the effects of G_{13}G225A on the ET-1-induced increase in $[Ca^{2+}]_i$ in CHO-ET_BR and CHO-SerET_BR. In this experiment, G_{13}G225A was microinjected into CHO-ET_BR and CHO-SerET_BR, and the ET-1-induced increase in $[Ca^{2+}]_i$ in these cells was analysed using microfluorimetry.

ET-1 failed to induce sustained increase in $[Ca^{2+}]_i$ in CHO-ET_BR microinjected with G_{13}G225A (Figure 7A) and CHO-SerET_BR microinjected with G_{13}G225A (Figure 7B). These results indicate that G_{13} plays critical roles in the activation of NSCC-1 and NSCC-2 caused by ET-1.

Effects of Y-27632 on the ET-1-induced sustained increase in $[Ca^{2+}]_i$ in CHO-ET_BR

It is generally accepted that Rho/Rho-kinase (ROCK) pathway is a downstream target of G_{13} (Seasholtz *et al*., 1999). We examined the effects of ROCK on ET-1-induced

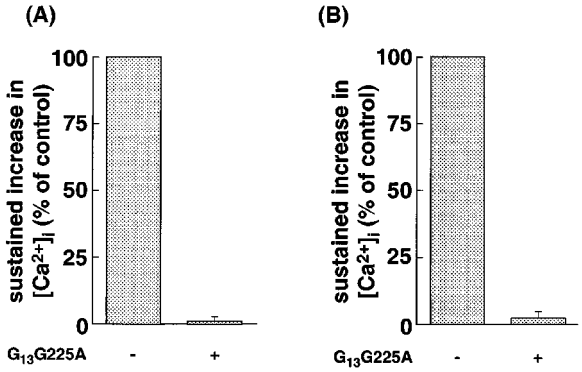

Figure 7 Effects of G_{13}G225A on ET-1-induced sustained increase in $[Ca^{2+}]_i$ in CHO-SerET_BR (A) and CHO-ET_BR (B). The cells loaded with fluo-3 were stimulated by 10 nM ET-1. The sustained increase in $[Ca^{2+}]_i$ in the presence of G_{13}G225A is represented as a percentage of values in its absence. Data are presented as mean$\pm$ s.e.m. of three experiments.

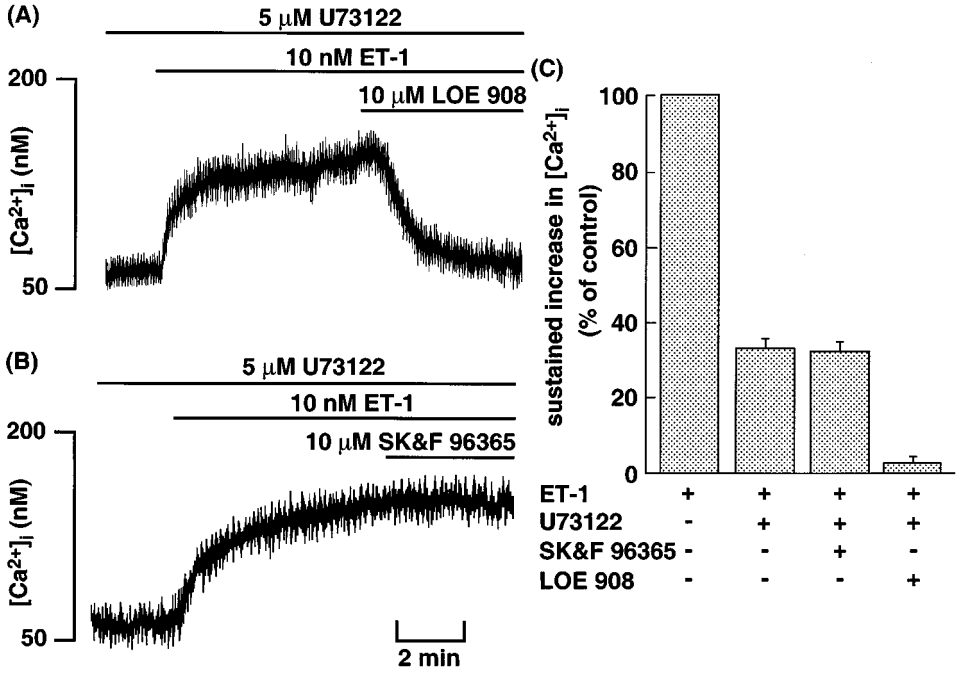

Figure 6 Original tracings illustrating the effects of maximally effective concentration of LOE 908 (A) and SK&F 96365 (B) on the ET-1-induced sustained increase in $[Ca^{2+}]_i$ in CHO-ET_BR pretreated with U73122. The cells loaded with fluo-3 were incubated with 5 μM U73122 for 10 min before 10 nM ET-1 stimulation. After $[Ca^{2+}]_i$ reached a steady-state, 10 μM LOE 908 or 10 μM SK&F 96365 was added at the time indicated by horizontal bars. (C) Effects of maximally effective concentration of LOE 908 and SK&F 96365 on the ET-1-induced sustained increase in $[Ca^{2+}]_i$ in CHO-ET_BR pretreated with U73122. The experimental protocols were described in Methods, and the values of $[Ca^{2+}]_i$ following addition of 10 μM LOE 908 or 10 μM SK&F 96365 were determined. Each point represents the mean$\pm$s.e.m. of five experiments.

increase in $[Ca^{2+}]_i$ in CHO-ET_BR. In this experiment, Y-27632 was used as a specific inhibitor of ROCK (Uehata *et al*., 1997). Y-27632 was added 15 min before stimulation with ET-1. Y-27632 at 10 μM did not affect the ET-1-induced transient and sustained increase in $[Ca^{2+}]_i$ (Figure 8).

Discussion

As reported previously (Kawanabe *et al*., 2001), the ET-1-induced sustained increase in $[Ca^{2+}]_i$ in CHO-ET_BR results from extracellular Ca^{2+} influx through two types of Ca^{2+}-permeable NSCC: NSCC-1 and NSCC-2 (Figures 4 & 5). The most important novelty of this study is that ET-1-induced NSCC-1 activation depends on G_{13}-dependent cascade, and NSCC-2 activation depends on both G_q/PLC- and G_{13}-dependent cascades in CHO-ET_BR.

To identify the G proteins involved in the activation of these Ca^{2+} channels by ET-1, we assessed whether G_{12} and G_{13} are coupled with CHO-ET_BR using actin stress fibre formation. A previous report demonstrated that G_q and G_{12}/G_{13} play important roles in the majority of GPCR-induced, Rho-mediated effects on the cytoskeleton (Seasholtz *et al*., 1999). Based on sensitivity to U73122, G_{12}G228A and G_{13}G225A (Figure 1), we conclude that ET-1-induced stress fiber formation is mediated *via* two signalling pathways in CHO-ET_BR (i.e., the G_q/PLC- and G_{13}-dependent pathways), and also that only one of the two may be sufficient for actin stress fibre formation. Moreover, G_i may not be involved in ET-1-induced stress fiber formation, because treatment of the cells with sufficient concentrations of PTX did not affect ET-1-induced actin stress fiber formation in CHO-ET_BR (Figure 1E). This result is in agreement with the previous indication that Rho-mediated effects on the cytoskeleton are PTX insensitive (Buhl *et al*., 1995). On the other hand, based on sensitivity to Y-27632, the Rho/ROCK pathway plays important roles in ET-1-induced stress fiber formation in CHO-ET_BR (Figure 1C) as reported for a variety of cells (Mao *et al*., 1998; Gohla *et al*., 1999; Seasholtz *et al*., 1999). Therefore, Rho/ROCK pathway may be downstream of both the G_q/PLC- and G_{13}-dependent pathways. We deduced the structural determinant for coupling of ET_BR with G_{13} based on data from experiments using mutated ET_BRs. That is, loss of coupling of $ET_BR\Delta403$ with G_{13} (Figure 3F) and retention of coupling of SerET_BR with G_{13} (Figure 2E) clearly show that the cytoplasmic tail downstream of Cys^{403} but not the palmitoylation site of ET_BR is essential for coupling with G_{13}. Judging from these data, we conclude that the cytoplasmic tail downstream of the palmitoylation sites of ET_BR, but not the palmitoylation site itself, is essential for coupling with G_{13}.

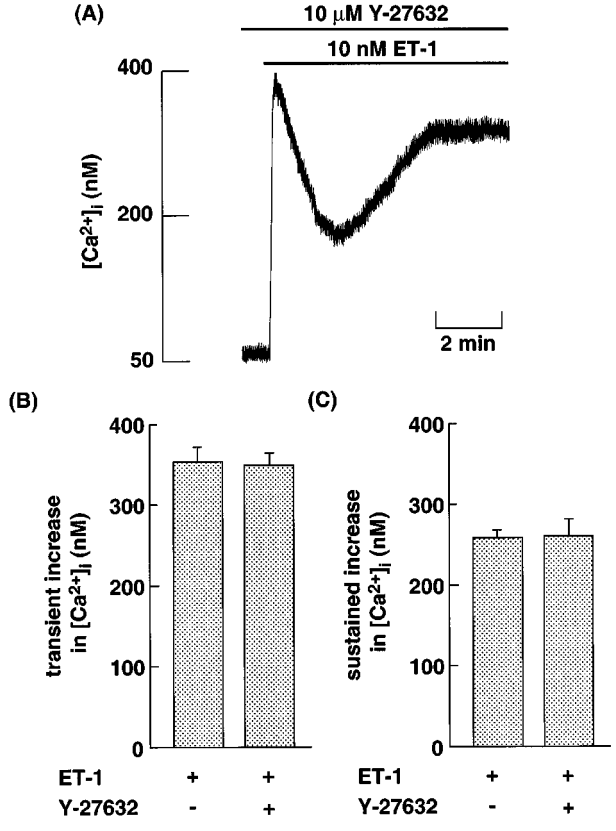

Figure 8 (A) Original tracing illustrating the effects of Y-27632 on the ET-1-induced increase in $[Ca^{2+}]_i$ in CHO-ET_BR. The cells loaded with fluo-3 were incubated with 10 μM Y-27632 for 15 min before 10 nM ET-1 stimulation. (B, C) Effects of 10 μM Y-27632 on 10 nM ET-1-induced transient (B) and sustained (C) increase in $[Ca^{2+}]_i$ in CHO-ET_BR. The experimental protocols were described in Methods. Data are presented as mean ± s.e.m. of three experiments.

Given that the subtypes of G proteins that are coupled with CHO-ET_BR has become clear, we analysed G proteins involved in the activation of NSCCs caused by ET-1. Judging from the data using U73122-treated CHO-ET_BR and CHO-$ET_BR\Delta403$ (Figures 4 & 6), G_q/PLC-independent pathways as well as G_q/PLC-dependent pathways are involved in NSCC-2 activation, while only G_q/PLC-independent pathways are involved in NSCC-1 activation. To elucidate the mechanism of NSCC-1 activation, we examined the effects of G_{13} using CHO-SerET_BR. ET-1-induced sustained increase in $[Ca^{2+}]_i$ is abrogated in CHO-SerET_BR microinjected with G_{13}G225A (Figure 7A). These results indicate that the G_{13}-dependent pathway seems to play an essential role for activation of NSCC-1 caused by ET-1. Moreover, these results support the indication that the cytoplasmic tail downstream of the palmitoylation sites of ET_BR, but not the palmitoylation site itself, is essential for coupling with G_{13}. Next, we examined the mechanisms of NSCC-2 activation using CHO-ET_BR microinjected with G_{13}G225A. ET-1 failed to induce sustained increase in $[Ca^{2+}]_i$ in these cells (Figure 7B). These results indicate that a G_{13}-dependent pathway plays an important role for activation of NSCC-2 as well as NSCC-1. In contrast, judging from the results using PTX, activation of NSCC-1 and NSCC-2 by ET-1 seems not to involve G_i-dependent pathway. In conclusion, NSCC-2 activation by ET-1 involves G_{13}-dependent pathway as well as G_q/PLC-dependent pathway. Recent reports demonstrated that G_{13} regulates cell growth (Seasholtz *et al*., 1999). Moreover, extracellular Ca^{2+} influx through NSCCs is involved in ET-1-induced cell proliferation in a variety of cells (Kawanabe *et al*., 2001; 2002). Therefore, G_{13} may be an effector for ET-1-induced cell proliferation by stimulating NSCCs. Collectively, among the subtypes of Gα proteins, G_q and G_{13} play important roles for activation of NSCCs as follows; (1) NSCC-1 activation involves a G_{13}-dependent

pathway. (2) NSCC-2 involves both G_q/PLC- and G_{13}-dependent pathways.

It is important to understand the mechanisms of ET-1 activation for each Ca^{2+} channel downstream of G_q and/or G_{13}. Because Rho/ROCK pathway is a downstream target of G_{13} (Seasholtz *et al*., 1999), we investigated the effects of ROCK on the activation of Ca^{2+} channels by ET-1 using a selective ROCK inhibitor, Y-27632. However, Y-27632 did not affect ET-1-induced increase in $[Ca^{2+}]_i$ (Figure 8). This result indicates that G_{13} activates NSCC-1 and NSCC-2 *via* ROCK-independent signaling pathways. Therefore, G_{13} may have another intracellular signalling pathway for activating NSCCs. Further study is needed to identify the effectors downstream of G_{13} for activation of NSCC-1 and NSCC-2.

We thank Boehringer Ingelheim K.G. for the kind donation of LOE 908. We also thank Welfide Corporation for the kind donation of Y-27632.

References

ARAI, H., HORI, S., ARAMORI, I., OHKUBO, H. & NAKANISHI, S. (1990). Cloning and expression of a cDNA encoding an endothelin receptor. *Nature,* **348,** 730 – 732.

ARAMORI, I. & NAKANISHI, S. (1992). Coupling of two endothelin receptor subtypes to differing signal transduction in transfected Chinese hamster ovary cells. *J. Biol. Chem.,* **267,** 12468 – 12474.

BETUING, S., DAVIAUD, D., PAGES, C., BONNARD, E., VALET, P., LAFONTAN, M. & SAULNIER-BLACHE, J.S. (1998). G$\beta\gamma$-independent coupling of α_2-adrenergic receptor to $p21^{rhoA}$ in preadipocytes. *J. Biol. Chem.,* **273,** 15804 – 15810.

BUHL, A.M., JOHNSON, N.L., DHANASEKARAN, N. & JOHNSON, G.L. (1995). G alpha 12 and G alpha 13 stimulate Rho-dependent stress fiber formation and focal adhesion assembly. *J. Biol. Chem.,* **270,** 24631 – 23634.

GOHLA, A., OFFERMANNS, S., WILKIE, T.M. & SCHULTZ, G. (1999). Differential involvement of Galpha12 and Galpha13 in receptor-mediated stress fiber formation. *J. Biol. Chem.,* **274,** 17901 – 17907.

GOHLA, A., SCHULTZ, G. & OFFERMANNS, S. (2000). Role of G12/G13 in agonist-induced vascular smooth muscle cell contraction. *Circ. Res.,* **87,** 221 – 227.

HORSTMEYER, A., CRAMER, H., SAUER, T., MULLER-ESTERL, W. & SCHROEDER, C. (1996). Palmitoylation of endothelin receptor A. Differential modulation of signal transduction activity by post-translational modification. *J. Biol. Chem.,* **271,** 20811 – 20819.

KAWANABE, Y., HASHIMOTO, N. & MASAKI, T. (2002). Ca^{2+} channels involved in endothelin-induced mitogenic response in carotid artery vascular smooth muscle cells. *Am. J. Physiol. Cell Physiol.,* **282,** C330 – C337.

KAWANABE, Y., OKAMOTO, Y., ENOKI, T., HASHIMOTO, N. & MASAKI, T. (2001). Ca^{2+} channels activated by endothelin-1 in CHO cells expressing endothelin-A or endothelin-B receptors. *Am. J. Physiol. Cell Physiol.,* **281,** C1676 – C1685.

KITAMURA, K., SHIRAISHI, N., SINGER, W.D., HANDLOGTEN, M.E., TOMITA, K. & MILLER, R.T. (1999). Endothelin-B receptors activate $G\alpha_{13}$. *Am. J. Physiol. Cell Physiol.,* **276,** C930 – C937.

MAO, J., YUAN, H., XIE, W., SIMON, M.I. & WU, D. (1998). Specific involvement of G proteins in regulation of serum response factor-mediated gene transcription by different receptors. *J. Biol. Chem.,* **273,** 27118 – 27123.

MASAKI, T. (1993). Endothelins: homeostatic and compensatory actions in the circulatory and endocrine systems. *Endocr. Rev.,* **14,** 256 – 268.

MINTA, A., KAO, J.P.Y. & TSIEN, R.Y. (1989). Fluorescent indicators for cytosolic calcium based on rhodamine and fluorescein chromophores. *J. Biol. Chem.,* **264,** 8171 – 8178.

OKAMOTO, Y., NINOMIYA, H., TANIOKA, M., SAKAMOTO, A., MIWA, S. & MASAKI, T. (1997). Palmitoylation of human $endothelin_B$. *J. Biol. Chem.,* **272,** 21589 – 21596.

SAKURAI, T., YANAGISAWA, M., TAKUWA, Y., MIYAZAKI, H., KIMURA, S., GOTO, K. & MASAKI, T. (1990). Cloning of cDNA encoding a non-isopeptide-selective subtype of the endothelin receptor. *Nature,* **348,** 732 – 735.

SEASHOLTZ, T.M., MAJUMDAR, M. & BROWN, J.H. (1999). Rho as a mediator of G protein-coupled receptor signaling. *Mol. Pharmacol.,* **55,** 949 – 956.

TAKAGI, Y., NINOMIYA, H., SAKAMOTO, A., MIWA, S. & MASAKI, T. (1995). Structural basis of G protein specificity of human endothelin receptors. A study with endothelinA/B chimeras. *J. Biol. Chem.,* **270,** 10072 – 10078.

UEHATA, M., ISHIZAKI, T., SATOH, H., ONO, T., KAWAHARA, T., MORISHIMA, T., TAMAKAWA, H., YAMAGAMI, K., INUI, J., MAEKAWA, M. & NARUMIYA, S. (1997). Calcium sensitization of smooth muscle mediated by a Rho-associated protein kinase in hypertension. *Nature,* **389,** 990 – 994.

YANAGISAWA, M., KURIHARA, S., KIMURA, S., TOMOBE, Y., KOBAYASHI, M., MITSUI, Y., YAZAKI, Y., GOTO, K. & MASAKI, T. (1988). A novel potent vasoconstrictor peptide produced by vascular endothelial cells. *Nature,* **332,** 411 – 415.

ZHANG, X.F., IWAMURO, Y., ENOKI, T., OKAZAWA, M., LEE, K., KOMURO, T., MINOWA, T., OKAMOTO, Y., HASEGAWA, H., FURUTANI, H., MIWA, S. & MASAKI, T. (1999). Pharmacological characterization of Ca^{2+} entry channels in endothelin-1-induced contraction of rat aorta using LOE 908 and SK&F 96365. *Br. J. Pharmacol.,* **127,** 1388 – 1398.

(Received March 6, 2002
Revised May 2, 2002
Accepted May 16, 2002)